analytical chemistry

Letter

pubs.acs.org/ac

Digital Polymerase Chain Reaction in an Array of Femtoliter Polydimethylsiloxane Microreactors

Yongfan Men,[†,‡] Yusi Fu,[†] Zitian Chen,[†,§] Peter A. Sims,[⊥,¶] William J. Greenleaf,[∥] and Yanyi Huang*[,†,‡,§]

[†]Biodynamic Optical Imaging Center (BIOPIC), School of Life Sciences, Peking University, Beijing 100871, China

[‡]College of Engineering, Peking University, Beijing 100871, China

[§]College of Chemistry and Molecular Engineering, Peking University, Beijing 100871, China

[⊥]Columbia Initiative in Systems Biology, Columbia University Medical Center, New York, New York 10032, United States

[¶]Department of Biochemistry and Molecular Biophysics, Columbia University Medical Center, New York, New York 10032, United States

[∥]Department of Genetics, Stanford University School of Medicine, Stanford, California 94305, United States

Supporting Information

ABSTRACT: We developed a simple, compact microfluidic device to perform high dynamic-range digital polymerase chain reaction (dPCR) in an array of isolated 36-femtoliter microreactors. The density of the microreactors exceeded 20 000/mm^2. This device, made from polydimethylsiloxane (PDMS), allows the samples to be loaded into all microreactors simultaneously. The microreactors are completely sealed through the deformation of a PDMS membrane. The small volume of the microreactors ensures a compact device with high reaction efficiency and low reagent and sample consumption. Future potential applications of this platform include multicolor dPCR and massively parallel dPCR for next generation sequencing library preparation.

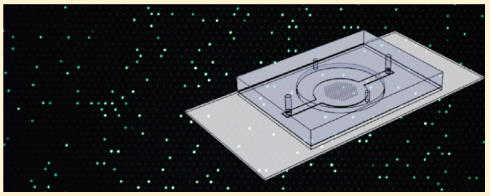

Digital polymerase chain reaction, or dPCR, employs parallel, isolated PCR reactions to amplify and/or quantify nucleic acids.[1,2] By amplifying templates in many separate reactions, each with typically one or zero templates, and then identifying the reactors with and without amplicons, the absolute number of template molecules can be counted without errors from amplification bias or noise. The identification of positive PCR reactions is usually based on TaqMan chemistry[3] due to high specificity and signal intensity of the fluorescence-based signal. Digital PCR, originally performed using multiwell plates, has been applied to assess the allelic imbalance, or loss of heterozygosity, in complex cell population such as tumors,[4−8] to quantitatively measure the concentration of DNA from human samples,[9] and to count cDNA templates in cancers.[10] Many methods, including statistical analysis[11,12] and multivolume digital assays,[13,14] have been applied to extend the dynamic range of dPCR.

With the help of microfluidic methods, dPCR becomes much easier to perform, requires less sample, and reduces contamination during experiments.[15−17] For example, the glass-based SlipChip provides a simple way to perform dPCR experiments.[18] Polydimethylsiloxane (PDMS)-based microfluidic devices with many microcompartments have been developed to carry dPCR experiments for single bacteria gene analysis,[19] single bacteria−virus infection detection,[20] single cell transcription profiling,[21,22] chromosomal aneuploidy detection,[23,24] copy number variation studies and validations,[25,26] absolute quantitative detection of rare mutations in cancers,[27−29] genetically modified food quantification,[30] and viral load monitoring.[31] The same method can be extended to other amplification technologies, such as multiple displacement amplification (MDA)[32] and loop-mediated amplification (LAMP).[33] Recently, with two-phase isolation, the density of microreactors for dPCR has been expanded to over 4400/mm^2 with picoliter compartments, greatly extending the dynamic range to seven logs with a large-scale chip format.[34] Another approach, which often employs microfluidics, involves the generation of microemulsions to isolate individual reactions.[35−39] Although this method is highly scalable,[40] the emulsion generation process and the reactions are cumbersome and the experiments usually require complex control apparatus.

We present a novel PDMS-based microfluidic device to perform dPCR in femtoliter microreactors. This device utilizes the elasticity of PDMS to create a high-density array of fully sealed and isolated microreactors through PDMS deformation[41,42] under hydraulic pressure.[43] This simple, space-saving design allows for a density of microreactors exceeding 20 000/mm^2 and allows rapid sample loading with a one-shot pipet injection of less than 4 μL of sample solution. Compared to previous nano- and picoliter approaches, our femtoliter-scale method reduces the number of thermal cycles required for detection, eliminating false positive counts. This design is

Received: March 18, 2012
Accepted: April 7, 2012

   dx.doi.org/10.1021/ac300761n | *Anal. Chem.* XXXX, XXX, XXX−XXX

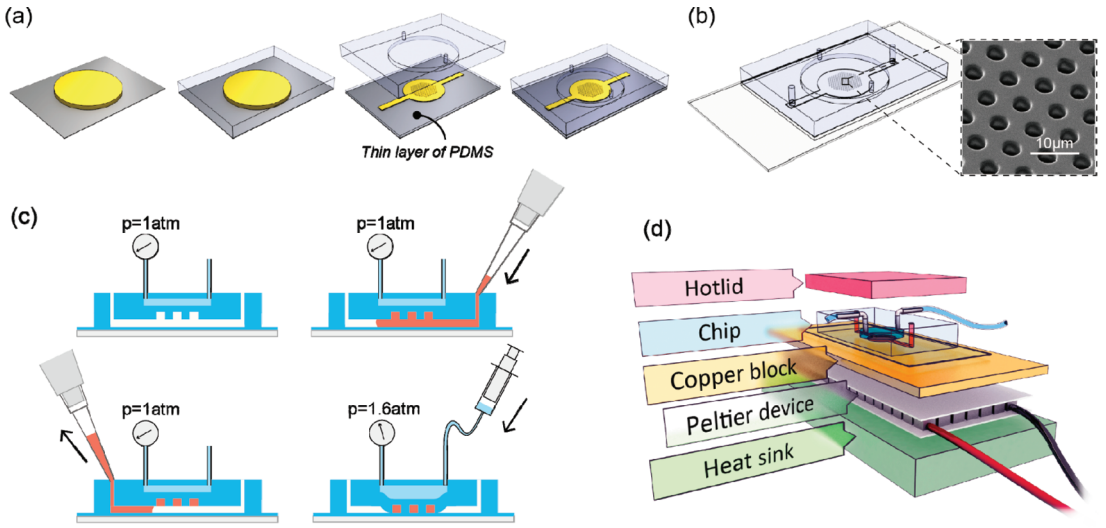

Figure 1. The fabrication, structure, and operation of the dPCR chip. (a) The fabrication procedure for the PDMS dPCR chip. Two molds, both generated through photolithography, are used to cast the two layers of chambers, respectively. The two PDMS slabs are bonded into a monolithic device. (b) The structure of the dPCR chip. The femtoliter microwells are fabricated in the bottom surface of the PDMS membrane between two chambers. The SEM image shows the dimension of the microwells. (c) The dPCR operation. The top chamber was filled with water, for compensating the loss of water during PCR thermal cycles. The sample was injected into the lower chamber to fill all the microwells. Excess sample was removed, and then, the top chamber was pressurized to seal and isolate all microreactors. (d) The thermocycler for dPCR. A Peltier device array, bonded with a copper block, was used to control the reaction temperature. The chip was placed directly onto the copper block.

intrinsically scalable, offering the possibility of performing dPCR with less sample consumption and a dynamic range of 10^5 with a 4 mm^2 array.

We employed multilayer soft lithography to fabricate the microfluidic dPCR chip with a high-density array of microwells (Figure 1a). The mold for the array is made from photoresist (SU-8, MicroChem) patterned with two-step photolithography on a silicon wafer. The chip has two layers of liquid chambers separated by a thin (1 mm), deformable PDMS membrane. The upper and lower chambers are 110 and 70 μm tall, respectively. The microwells are in the bottom surface of this membrane. Each well is 3.3 $\pm$ 0.1 μm in diameter and 4.2 $\pm$ 0.1 μm deep, with a volume of 36 $\pm$ 2 fL (Figures 1b and S3, Supporting Information). We fabricated a hexagonally close packed array with a period of 7.5 μm containing 82 000 wells within a 2 $\times$ 2 mm array area.

As shown in Figure 1c, we loaded the sample solution into the lower chamber with a pipet, and then, excess solution was removed by evacuating the liquid from the outlet of the chamber before actuating the membrane. Without this evacuation step, excess liquid in the lower chamber can cause imperfect sealing upon membrane deformation and eventually lead to the unreliable quantification. With positive pressure applied to the upper chamber, the PDMS membrane deforms to seal all the microwells, creating isolated microreactors. To prevent evaporation through the water-permeable PDMS membrane, we loaded the upper chamber with water (~5 μL). We found that our method to prevent evaporation was insufficient if the thickness of the PDMS membrane exceeded 1 mm. The bottom of the lower chamber is a coverslip coated with a 10 μm PDMS layer. The hydrophobic nature of this PDMS layer enhances the sealing of the microreactors. The performance of sealing is evaluated and confirmed though a photobleaching test before each experiment. Fluorescein solution is sealed into the reactors, and a portion of the field of view is illuminated with the laser for a lengthy exposure time. A few minutes after exposure, we take wide-field fluorescence images (Figure S4, Supporting Information). If the microreactors are well-sealed, a photobleached area can be clearly observed; otherwise, the bleaching pattern vanishes because dyes diffuse between the microreactors.

We built a customized thermocycling system (Figure 1d) for our dPCR chip. This system uses four Peltier devices (TE-31-1.4-1.15R, TE Technology, Inc.) connected in series underneath the chip to control the temperature of microreactors. We also apply another Peltier device to keep the top of the device at 95 °C. This hot lid increases the temperature ramping rate and also helps prevent evaporation. The pressure (170 kPa) of the upper water chamber was constantly monitored using an electronic pressure sensor to ensure the microreactors were well-sealed during the experiment. After loading the sample and confirming the seal, we placed the chip on our dPCR thermocycler. Samples were typically run for 30 two-step cycles (5 s at 90 °C and 20 s at 55 °C) with an initial denaturing step (60 s at 90 °C, 60 s at 55 °C, 60 s at 90 °C, and 60 s at 55 °C) for the reaction. The entire experiment is completed within ~35 min.

After dPCR thermocycles, we transferred the chip to an inverted fluorescence microscope (Ti-E, Nikon) with a 20× N.A. 0.75 objective for observation. We used TaqMan probes to detect the individual PCR reactions in each microreactor. Amplified target template within a microreactor generates fluorescent dye that is confined within the microreactor. Microreactors that are positive for template amplification can be detected within 30 amplification cycles.

Fluorescence images were captured with a scientific CMOS camera (Neo-DC-152Q-FI, Andor), and each field-of-view contained 11 855 microreactors (825 mm × 700 mm, ~70 pixels/microreactor). Each array was fully quantified with 9 images. The fluorescence was excited by a 473 nm DPSS CW laser, and the power density at the focal plane was 13 mW/mm^2. Figure 2a shows a typical dPCR image with ~3100 microreactors. After 30 dPCR cycles, the microreactors with zero copies of template exhibit a small amount of residual

dx.doi.org/10.1021/ac300761n | Anal. Chem. XXXX, XXX, XXX–XXX

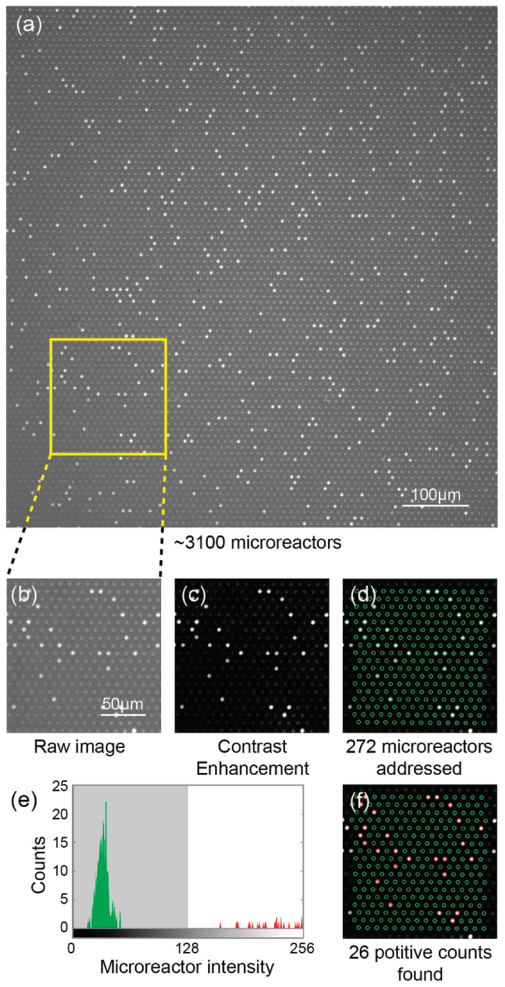

Figure 2. The dPCR quantification pipeline. (a) A region of a raw experimental image containing ~3100 microreactors. (b) A region of interest with 272 microreactors. (c) Bright PCR microreactors can be distinguished from dark microreactors after contrast enhancement (see text). (d) Locations of the microreactors are determined. (e) A histogram of the integrated intensity from each microreactor. (f) 26 microreactors are found to be positive.

fluorescence, due to the autofluorescence of PDMS and the background of the TaqMan probe, which is significantly weaker than the fluorescence generated by TaqMan probes in the positive microreactors. We used a top-hat filter to subtract much of this background and enhance the contrast (Figure 2c). The hexagonal alignment of the microreactors allows for simple segmentation (Figure 2d), and the integrated intensities from bright and dark reactors are well-separated (Figure 2e), allowing digital identification of reactors that were positive and negative for template amplification (Figure 2f). This quantification pipeline provides the absolute number of amplicon-containing microreactors, as well as the ratio between the positive counts and the total number of microreactors.

To achieve robust and quantitative dPCR results, proper surface treatment of the microreactors is required. Hydrophobic macromolecules and fluorophores can adsorb to bare PDMS surfaces. Because of the large surface area to volume ratio of the femtoliter microreactors, surface adsorption is an especially acute possibility and could severely hinder the efficiency of PCR. We passivated the microreactors by soaking the lower chamber with the reaction buffer without template for 30 min and air drying the chamber before loading the sample.

To test our dPCR chip, we synthesized an 88 nt template sequence, from the mouse homeobox A1 gene (*Hoxa1*), and prepared standard solutions with the final concentration ranging from 1.25 to 20 pM. Each sample was tested 3 times, and each experiment was performed on a newly prepared chip. Figure 3a shows two sets of the experimental results. As the template concentration increases, we observed more positive microreactors under the microscope. The bright microreactors are randomly distributed, but the ratios between the positive

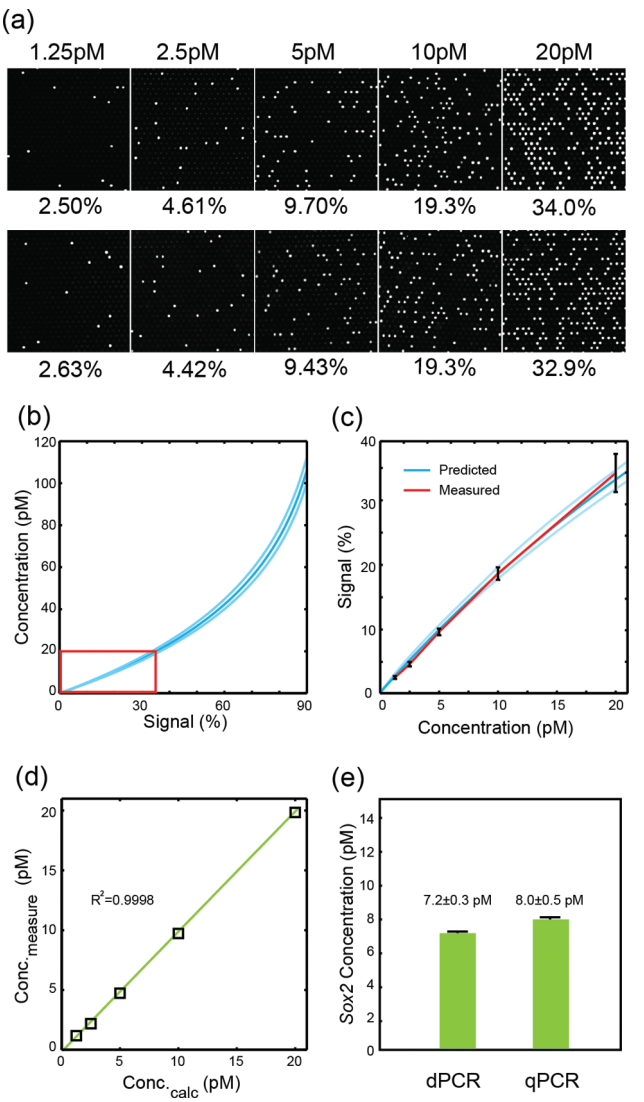

Figure 3. dPCR experimental results (a) Two independent sets of experiments of dPCR with 5 different concentrations of templates. The percentage of the counts of each experiment is shown. (b) The concentration of the templates can be calcualted from the fraction of positive microreactors. The thick blue curve is the theoretical result calculated from Poisson statistics. The two thin curves indicated the uncertainties of the calculation due to uncertainties in the volume measurement of the microreactors. (c) The measured fraction of positive microreactors match well with the predicted values according to Poisson statistics. (d) The correlation between the measured concentration and the prepared concentration of cDNA templates. (e) The quantitative real-time PCR and dPCR quantifications of concentrations of *Sox2* gene cDNAs.

dx.doi.org/10.1021/ac300761n | *Anal. Chem.* XXXX, XXX, XXX–XXX

counts and the total number of microreactors are consistent in different experimental runs, indicating the robustness of the dPCR chip.

The relationship between the concentration and the expected fraction of positive reactors from Poisson statistics is shown in Figure 3b. Given the measured fraction of positive reactors, we can calculate the absolute number of molecules within all the reaction volumes and, therefore, the concentration of template in the solution. Our experimental results are consistent with the theoretical curve, as shown in Figure 3c. We tested the accuracy of our dPCR system by calculating the correlation between the measured concentration of template from digital counting and the prepared concentration from serial dilutions. The correlation between the two sets of values is 0.9998.

We then prepared a cDNA solution through reverse transcription of total RNA extracted from 1.4×10^5 cells (mouse embryonic stem cells). We applied our dPCR chips to measure the concentration of mouse SRY-box containing gene 2 (*Sox2*), the gene of the key transcription factor that is essential to the self-renewal capacity of embryonic stem cells, from the sample, and compared the result with conventional q-PCR. As indicated in Figure 3e, the concentration was measured to be 7.2 ± 0.3 pM from dPCR and 8.0 ± 0.5 pM from q-PCR.

The high-density microfluidic dPCR platform described here has a number of advantages over other dPCR platforms. The increased density of the array allows us to reach a dynamic range of almost 5 logs with a small sample volume on a tiny chip. Compared with most previous reports, in which 40 or more temperature cycles were typically applied to picoliter or larger reactors, our femtoliter microreactors greatly increase the effective concentration of template and consequently reduce the number of cycles needed. A typical practice in dPCR experiments is to prepare the extremely dilute samples to guarantee that the template copy number in each isolated reactor is reasonably low, enabling the digital counting. Shrinking the size of the microreactors creates the possibility of the use of samples without further dilution, eliminating possible contamination and error during the extra experimental steps. With the greatly reduced volume of each microreactor, we can directly use the samples with picomolar concentrations to perform the experiments. Additionally, compared with many other approaches such as emulsion and larger chips with microchambers, our method requires less time and effort to create a large number of isolated reactors. Many reactions can be integrated into a single device, and the image can be acquired by a scanning-based detection system, which has been widely used for microarrays and DNA sequencers.

The digital counting result can also be exploited to provide the absolute counts of expressed mRNA number of certain genes. In our case, the average number of expressed *Sox2* mRNAs was 3.2×10^2 copies/cell. The ability to count the absolute number of mRNA molecules also demonstrates the possibility of single cell measurements, which will become one of the most important applications of dPCR. The PDMS microreactor array can be seamlessly integrated with other functional components in a single chip for screening, handling, and processing individual cells. Microfluidic integration will greatly increase reproducibility while reducing contamination. In addition, because quantification is based on a microscopic readout, this platform can be easily extended to multicolor dPCR for simultaneous measurements of multiple genes of interest.

Finally, this high-density platform may have applications to high-throughput sequencing sample preparation. High-throughput sequencing libraries are often preamplified using common sequencing primers ligated to a heterogeneous population of DNA fragments to generate a diverse set of DNA fragments to sequence. However, differences in amplification efficiency can cause the relative abundances of different DNA fragments to change.[44,45] By carrying out this amplification step in microreactors and running the dPCR reaction to completion, we anticipate that this nonlinear amplification bias will be mitigated, as every equally sized reaction chamber will generate an approximately equal number of DNA fragments. This DNA can be recovered by unsealing the reactors and flowing out the products. Such digital amplification will eliminate the biases inherent in bulk multiplex PCR and allow for a more quantitative readout of nucleic acid copy number using sequencing methods.

In summary, we have reported a novel microfluidic device with an array of femtoliter microreactors that can be simply sealed and isolated for digital PCR experiments. The 36 fL microreactors are arrayed at high density, allowing us to reach more than 20 000 reactors/mm^2. We characterized the performance of the dPCR on-chip and employed this device to test the cDNA sample that was reverse-transcribed from embryonic stem cells. We have demonstrated that this method is robust and reproducible for achieving high dynamic-range dPCR reactions with high efficiency, limited sample volume, and without extensive dilutions. This method is also easily scalable to millions of microreactors within a square centimeter using existing technology and may be extended to multicolor dPCR and to highly multiplexed dPCR reactions.

■ ASSOCIATED CONTENT

Supporting Information

Additional information as noted in text. This material is available free of charge via the Internet at http://pubs.acs.org.

■ AUTHOR INFORMATION

Corresponding Author

*E-mail: yanyi@pku.edu.cn.

Notes

P.A.S. and W.J.G. are listed as inventors on a patent application based on this work filed by Harvard University.

■ ACKNOWLEDGMENTS

The authors thank Hongshan Guo and Prof. Fuchou Tang for providing samples, Tao Chen for SRS microscopy, and Prof. X. Sunney Xie for fruitful discussion. This work was supported by the National Natural Science Foundation of China (90913011), the Ministry of Science and Technology of China (2011CB809106), and the Fok Ying Tung Education Foundation.

■ REFERENCES

(1) Vogelstein, B.; Kinzler, K. W. *Proc. Natl. Acad. Sci. U.S.A.* **1999**, *96*, 9236−9241.
(2) Pohl, G.; Shih, I. M. *Expert Rev. Mol. Diagn.* **2004**, *4*, 41−47.
(3) Holland, P. M.; Abramson, R. D.; Watson, R.; Gelfand, D. H. *Proc. Natl. Acad. Sci. U.S.A.* **1991**, *88*, 7276−7280.
(4) Shih, I. M.; Zhou, W.; Goodman, S. N.; Lengauer, C.; Kinzler, K. W.; Vogelstein, B. *Cancer Res.* **2001**, *61*, 818−822.

(5) Zhou, W.; Galizia, G.; Lieto, E.; Goodman, S. N.; Romans, K. E.; Kinzler, K. W.; Vogelstein, B.; Choti, M. A.; Montgomery, E. A. *Nat. Biotechnol.* **2001**, *19*, 78−81.
(6) Chang, H. W.; Ali, S. Z.; Cho, S. K.; Kurman, R. J.; Shih, I, M. *Clin. Cancer Res.* **2002**, *8*, 2580−2585.
(7) Chang, H. W.; Lee, S. M.; Goodman, S. N.; Singer, G.; Cho, S. K.; Sokoll, L. J.; Montz, F. J.; Roden, R.; Zhang, Z.; Chan, D. W.; Kurman, R. J.; Shih, I, M. *J. Natl. Cancer Inst.* **2002**, *94*, 1697−1703.
(8) Zhou, W.; Goodman, S. N.; Galizia, G.; Lieto, E.; Ferraraccio, F.; Pignatelli, C.; Purdie, C. A.; Piris, J.; Morris, R.; Harrison, D. J.; Paty, P. B.; Culliford, A.; Romans, K. E.; Montgomery, E. A.; Choti, M. A.; Kinzler, K. W.; Vogelstein, B. *Lancet* **2002**, *359*, 219−225.
(9) Traverso, G.; Shuber, A.; Olsson, L.; Levin, B.; Johnson, C.; Hamilton, S. R.; Boynton, K.; Kinzler, K. W.; Vogelstein, B. *Lancet* **2002**, *359*, 403−404.
(10) Yan, H.; Dobbie, Z.; Gruber, S. B.; Markowitz, S.; Romans, K.; Giardiello, F. M.; Kinzler, K. W.; Vogelstein, B. *Nat. Genet.* **2002**, *30*, 25−26.
(11) Warren, L. A.; Weinstein, J. A.; Quake, S. R., 2007, pp 1−9; http://thebigone.stanford.edu/papers/Weinstein%20DigResCurve.pdf (Accessed 2007).
(12) Dube, S.; Qin, J.; Ramakrishnan, R. *PLoS One* **2008**, *3*, e2876.
(13) Kreutz, J. E.; Munson, T.; Huynh, T.; Shen, F.; Du, W.; Ismagilov, R. F. *Anal. Chem.* **2011**, *83*, 8158−8168.
(14) Shen, F.; Sun, B.; Kreutz, J. E.; Davydova, E. K.; Du, W.; Reddy, P. L.; Joseph, L. J.; Ismagilov, R. F. *J. Am. Chem. Soc.* **2011**, *133*, 17705−17712.
(15) Piggee, C. *Anal. Chem.* **2007**, *79*, 8828.
(16) Sundberg, S. O.; Wittwer, C. T.; Gao, C.; Gale, B. K. *Anal. Chem.* **2010**, *82*, 1546−1550.
(17) Zhang, C.; Xing, D. *Chem. Rev.* **2010**, *8*, 4910−4947.
(18) Shen, F.; Du, W.; Kreutz, J. E.; Fok, A.; Ismagilov, R. F. *Lab Chip* **2010**, *10*, 2666−2672.
(19) Ottesen, E. A.; Hong, J. W.; Quake, S. R.; Leadbetter, J. R. *Science* **2006**, *314*, 1464−1467.
(20) Tadmor, A. D.; Ottesen, E. A.; Leadbetter, J. R.; Phillips, R. *Science* **2011**, *333*, 58−62.
(21) Warren, L.; Bryder, D.; Weissman, I. L.; Quake, S. R. *Proc. Natl. Acad. Sci.* **2006**, *103*, 17807−17812.
(22) Tay, S.; Hughey, J. J.; Lee, T. K.; Lipniacki, T.; Quake, S. R.; Covert, M. W. *Nature* **2010**, *466*, 267−271.
(23) Fan, H. C.; Quake, S. R. *Anal. Chem.* **2007**, *79*, 7576−7579.
(24) Fan, H. C.; Blumenfeld, Y. J.; El-Sayed, Y. Y.; Chueh, J.; Quake, S. R. *Am. J. Obstet. Gynecol.* **2009**, *200*, e1−e7.
(25) Qin, J.; Jones, R. C.; Ramakrishnan, R. *Nucleic Acids Res.* **2008**, *36*, e116.
(26) Pushkarev, D.; Neff, N. F.; Quake, S. R. *Nat. Biotechnol.* **2009**, *27*, 847−850.
(27) Oehler, V. G.; Qin, J.; Ramakrishnan, R.; Facer, G.; Ananthnarayan, S.; Cummings, C.; Deininger, M.; Shah, N.; Mccormick, F.; Willis, S.; Daridon, A.; Unger, M.; Radich, J. P. *Leukemia* **2009**, *23*, 396−399.
(28) Yung, T. K.; Chan, K. C.; Mok, T. S.; Tong, J.; To, K. F.; Lo, Y. M. *Clin. Cancer Res.* **2009**, *15*, 2076−2084.
(29) Wang, J.; Ramakrishnan, R.; Tang, Z.; Fan, W.; Kluge, A.; Dowlati, A.; Jones, R. C.; Ma, P. C. *Clin. Chem.* **2010**, *56*, 623−632.
(30) Corbisier, P.; Bhat, S.; Partis, L.; Xie, V. R.; Emslie, K. R. *Anal. Bioanal. Chem.* **2010**, *396*, 2143−2150.
(31) White Iii, R. A.; Quake, S. R.; Curr, K. *J. Virol. Methods* **2011**, *1*, 45−50.
(32) Blainey, P. C.; Quake, S. R. *Nucleic Acids Res.* **2011**, *39*, e19.
(33) Gansen, A.; Herrick, A. M.; Dimov, I. K.; Lee, L. P.; Chiu, D. T. *Lab Chip* **2012**, DOI: 10.1039/C2LC21247A.
(34) Heyries, K. A.; Tropini, C.; Vaninsberghe, M.; Doolin, C.; Petriv, O. I.; Singhal, A.; Leung, K.; Hughesman, C. B.; Hansen, C. L. *Nat. Methods* **2011**, *8*, 649−651.
(35) Hatch, A. C.; Fisher, J. S.; Pentoney, S. L.; Yang, D. L.; Lee, A. P. *Lab Chip* **2011**, *11*, 2509−2517.
(36) Hindson, B. J.; Ness, K. D.; Masquelier, D. A.; Belgrader, P.; Heredia, N. J.; Makarewicz, A. J.; Bright, I. J.; Lucero, M. Y.; Hiddessen, A. L.; Legler, T. C.; Kitano, T. K.; Hodel, M. R.; Petersen, J. F.; Wyatt, P. W.; Steenblock, E. R.; Shah, P. H.; Bousse, L. J.; Troup, C. B.; Mellen, J. C.; Wittmann, D. K.; Erndt, N. G.; Cauley, T. H.; Koehler, R. T.; So, A. P.; Dube, S.; Rose, K. A.; Montesclaros, L.; Wang, S.; Stumbo, D. P.; Hodges, S. P.; Romine, S.; Milanovich, F. P.; White, H. E.; Regan, J. F.; Karlin-Neumann, G. A.; Hindson, C. M.; Saxonov, S.; Colston, B. W. *Anal. Chem.* **2011**, *83*, 8604−8610.
(37) Pinheiro, L. B.; Coleman, V. A.; Hindson, C. M.; Herrmann, J.; Hindson, B. J.; Bhat, S.; Emslie, K. R. *Anal. Chem.* **2012**, *84*, 1003−1011.
(38) Qi, Z.; Ma, Y.; Deng, L.; Wu, H.; Zhou, G.; Kajiyama, T.; Kambara, H. *Analyst* **2011**, *136*, 2252−2259.
(39) Zhong, Q.; Bhattacharya, S.; Kotsopoulos, S.; Olson, J.; Taly, V.; Griffiths, A. D.; Link, D. R.; Larson, J. W. *Lab Chip* **2011**, *11*, 2167−2174.
(40) Hatch, A. C.; Fisher, J. S.; Tovar, A. R.; Hsieh, A. T.; Lin, R.; Pentoney, S. L.; Yang, D. L.; Lee, A. P. *Lab Chip* **2011**, *11*, 3838−3845.
(41) Sims, P. A.; Greenleaf, W. J.; Duan, H.; Xie, X. S. *Nat. Methods* **2011**, *8*, 575−580.
(42) Gong, Y.; Ogunniyi, A. O.; Love, J. C. *Lab Chip* **2010**, *10*, 2334−2337.
(43) Unger, M. A. *Science* **2000**, *288*, 113−116.
(44) Aird, D.; Ross, M. G.; Chen, W. S.; Danielsson, M.; Fennell, T.; Russ, C.; Jaffe, D. B.; Nusbaum, C.; Gnirke, A. *Genome Biol.* **2011**, *12*, R18.
(45) Shiroguchi, K.; Jia, T. Z.; Sims, P. A.; Xie, X. S. *Proc. Natl. Acad. Sci. U.S.A.* **2012**, *109*, 1347−1352.